John S. H. Tang, MD • Richard H. Gold, MD • Lawrence W. Bassett, MD
• Leanne L. Seeger, MD

Musculoskeletal Infection of the Extremities: Evaluation with MR Imaging[1]

Magnetic resonance (MR) imaging was performed in 17 patients, 11–84 years of age, referred for evaluation of possible osteomyelitis involving the appendicular skeleton. MR imaging permitted successful identification of osteomyelitis in ten patients (four acute, two subacute with Brodie abscess, two chronic, and two acute with septic arthritis) and of cellulitis in the absence of osteomyelitis in four patients, including one with a soft-tissue abscess. Active osteomyelitis was excluded in three patients. Both T1- and T2-weighted spin-echo sequences were needed to evaluate osteomyelitis. T2-weighted images were needed to identify foci of active infection. MR images provided more accurate and detailed information regarding the extent of involvement than did radionuclide bone scans, computed tomographic scans, or standard radiographs. It permitted the differentiation of septic arthritis or cellulitis from osteomyelitis. In this limited series, MR imaging was particularly useful for seeking foci of active infection in areas of chronic osteomyelitis complicated by surgical intervention or fracture.

RADIOLOGIC diagnosis of osteomyelitis remains a problem that is rendered even more difficult when underlying bone abnormalities, such as deformities from previous trauma or surgery, are also present. In the earliest stage of osteomyelitis, conventional radiographs may be normal. Although technetium-99m–labeled methylene diphosphonate (MDP) bone scanning has been recognized as the most sensitive imaging study for the early detection of osteomyelitis, it is nonspecific and the findings are often equivocal (1–4). Computed tomographic (CT) scanning has proved to be a useful adjunct to conventional radiography and radionuclide studies in the evaluation of selected patients who may have bone or joint infections (5). CT is capable of depicting sequestra, cloacae, sinus tracts, foreign bodies, and intramedullary and soft-tissue gas (6, 7). However, CT scans may provide only limited information in patients with metallic joint prostheses or internal fixation devices.

Because of its proved capability in the demonstration of anatomic details and its high sensitivity in the detection of pathologic changes in the bone marrow, magnetic resonance (MR) imaging has been recognized as a useful imaging modality in the evaluation of musculoskeletal disease. Although the number of patients described thus far has been small, preliminary evaluation has shown MR imaging to have a high sensitivity in the detection of the presence and the local extent of infections of the musculoskeletal system (3, 4, 8–16). One study found MR imaging to be more sensitive and more specific than either radionuclide bone scanning or plain radiography in the evaluation of vertebral osteomyelitis (12). We attempt herein to define the role and the limitations of MR imaging in the evaluation of infections of the extremities.

MATERIALS AND METHODS

Seventeen consecutive patients, 11–84 years of age (average age, 44 years), were referred for MR imaging evaluation of possible osteomyelitis of an extremity. In all patients standard radiographs of the involved site were obtained, CT scans were obtained in three (3–10-mm-thick sections, bolus of intravenously administered contrast material), ten underwent single-phase Tc-99m MDP bone scanning, and two of these ten patients also underwent indium-111–labeled leukocyte scanning. The sites studied with MR imaging included the shoulder, humerus, hip, femur, knee, tibia, fibula, ankle, and foot. Twelve patients underwent surgery within 1 week of MR imaging examination. All surgical specimens were referred for histologic and bacteriologic culture examinations.

Fifteen patients were imaged with a 0.3-T permanent magnet, Beta 3000 system (Fonar, Melville, N.Y.) (256 × 256 matrix, 5-mm-thick sections at 7-mm intervals, four excitations averaged), one was imaged with a 1.5-T superconductive magnet, Signa system (General Electric Medical, Milwaukee), and one was imaged with a 0.15-T resistive magnet system (Picker, Highland Heights, Ohio). To improve image quality, surface coils were used whenever possible. When a comparison with the normal side was needed, both sides of the body were imaged simultaneously. Fourteen patients were studied with two spin-echo (SE) pulse sequences: a T1-weighted sequence (500–800/28) (repetition time [TR] msec/echo time [TE] msec) and a T2-weighted sequence (1,500–2,000/56–84). Three patients were examined with one sequence only, two patients with a T1-weighted sequence only, and one with a T2-weighted sequence only. Axial and coronal images were obtained on a 256 × 256 matrix, with a 5–9-mm section thickness and 0.75-mm pixels. Sagittal images were obtained when necessary. Interpretation of the images was done prospectively but with full knowledge of clinical data and results of other imaging modalities.

RESULTS

On the basis of features seen on MR images, oestomyelitis was correctly di-

agnosed in ten of the 17 patients (Figs. 1–5): four had acute osteomyelitis alone, two had septic arthritis and associated acute osteomyelitis, two had subacute osteomyelitis with a Brodie abscess, one had chronic osteomyelitis with a sequestrum, and one had a reactivation of chronic osteomyelitis. The MR imaging examinations of the seven remaining patients revealed no musculoskeletal infections: one study depicted healed osteomyelitis in combination with a healed pyarthrosis, three showed only cellulitis, three depicted only a soft-tissue abscess (Fig. 6), one revealed a healed, noninfected tibial fracture, and one illustrated noninfected Gaucher disease and bone infarcts. Twelve diagnoses were confirmed with surgical exploration and pathologic and bacteriologic examination, while five were determined on the basis of correlation with the clinical course and other available imaging studies. Although MR images correctly depicted changes characteristic of active osteomyelitis in ten of ten cases, the biased patient selection and limited number of cases prevent us from making a meaningful determination of the sensitivity and specificity of MR imaging in the diagnosis of osteomyelitis.

A single-phase Tc-99m MDP bone scan was obtained in ten patients and showed increased uptake in five of the six patients with active osteomyelitis. Scan findings were also positive in one patient with a healed fracture of the tibia and in two patients with cellulitis, none of whom had associated osteomyelitis. In-111–labeled leukocyte scanning was performed in two patients, both with active chronic osteomyelitis, but findings were positive in only one.

CT scanning was performed in two patients with chronic osteomyelitis and in one with a Brodie abscess. In the two patients with chronic osteomyelitis, CT successfully demonstrated a sequestrum in one, and a cloaca and sinus tract in the other (Fig. 4). In the patient with a Brodie abscess, CT disclosed the abscess cavity (Fig. 5).

In the six patients with acute osteomyelitis, conventional radiographs were suggestive of osteomyelitis, disclosing bone resorption, adjacent soft-tissue swelling, and periosteal new bone formation; a narrowed joint space was found in a patient with associated septic arthritis of the hip. In the two cases of Brodie abscess a cystlike focus of destruction, well-demarcated by a sclerotic rim, was a characteristic radiographic finding. However, radiographs were not helpful in evaluating chronic osteomyelitis, since they were unable to demonstrate either sequestra or findings suggestive of active infection. Mild to moderate soft-tissue swelling with or without periosteal new bone

was shown in the four patients with soft-tissue infection. In the three patients without osteomyelitis or soft-tissue infection the radiographs did not suggest osteomyelitis or soft-tissue inflammation.

The changes identified with MR imaging in all 17 patients are summarized as follows:

Acute osteomyelitis (four patients).— Sites of involved medullary bone appeared on T1-weighted images as areas of ill-defined and homogeneous low-to-intermediate signal intensity and on T2-weighted images as areas of high signal intensity, as bright as or brighter than bone marrow. On T1-weighted images there were accompanying areas of ill-defined intermediate signal intensity in the cortex and soft tissue and disruption of the normal high-intensity signal of the adjacent intermuscular septa and subcutaneous fat. These foci changed to high signal intensity on T2-weighted images, just as the lesions in the medullary canal had.

Subacute osteomyelitis with Brodie abscess (two patients).—Intraosseous and extraosseous abscesses were of low-to-intermediate intensity on T1-weighted images and became brighter than normal marrow on T2-weighted images. An intraosseous abscess was well-demarcated by a low-intensity rim on both T1- and T2-weighted images (Fig. 5). One of the abscess cavities contained a sequestrum seen on T2-weighted images as an area of low intensity (Fig. 6).

Chronic osteomyelitis (two patients).— The abnormal medullary bone appeared inhomogeneous. Foci of exudate were characterized as well-defined lesions with or without a low-intensity rim, the changes in signal intensity being similar to those characterizing Brodie abscess. Sequestra, involucra, and sinus tracts appeared as foci of low-to-intermediate signal intensity that did not change significantly on T1- to T2-weighted images (Fig. 4). Likewise, underlying old fractures or surgical scars appeared as foci of low-to-intermediate signal intensity on both T1- and T2-weighted sequences.

Acute osteomyelitis with septic arthritis (two patients).—The abnormal medullary cavity, cortex, and soft tissue manifested changes in signal intensity similar to those seen in acute osteomyelitis. In addition, excessive fluid in joints and bursae appeared as areas of strikingly high signal intensity on T2-weighted images. When severe thinning of articular cartilage was present, the joint space on T2-weighted images appeared lower in signal intensity and more distinct than the space in the contralateral normal joint (Fig. 3b).

Healed, inactive osteomyelitis with healed pyarthrosis (one patient).—No ab-

a.

b.

Figure 1. Images in 76-year-old man with acute osteomyelitis of right tibia and soft-tissue abscess of left tibia. (a) Anteroposterior radiograph of area of interest in right tibia reveals soft-tissue swelling and subtle irregularity of the cortex below the medial tibial condyle, which suggests periosteal reaction. (b) Coronal MR image of right knee (SE 500/28) reveals lesion in tibia manifesting homogeneous decrease in signal intensity and irregular margin. Adjacent cortex and soft tissues have abnormal, slightly increased signal intensity.
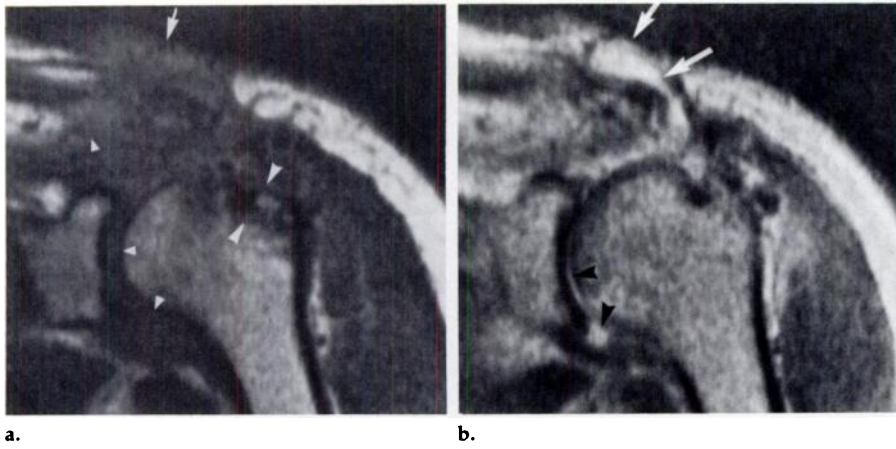
Figure 2. MR images in 53-year-old man with osteomyelitis of humerus and postsurgical septic arthritis of shoulder. (a) Coronal image (SE 500/28) depicts ill-defined, low-intensity lesion of greater tuberosity of humerus (large arrowheads). Large focus of abnormal intermediate signal intensity involves regional soft tissue, acromioclavicular joint, and axillary recess (small arrowheads). Normally bright subcutaneous fat is interrupted (arrow). (b) Coronal image (SE 1,999/58). Homogeneous increase in signal intensity is present in greater tuberosity, and high-intensity effusion in glenohumeral joint and axillary recess (arrowheads). Diffuse, ill-defined increase in signal intensity is also present at acromioclavicular joint and in regional soft tissue. Bright, well-defined draining sinus tract characterizes pus content (arrows).
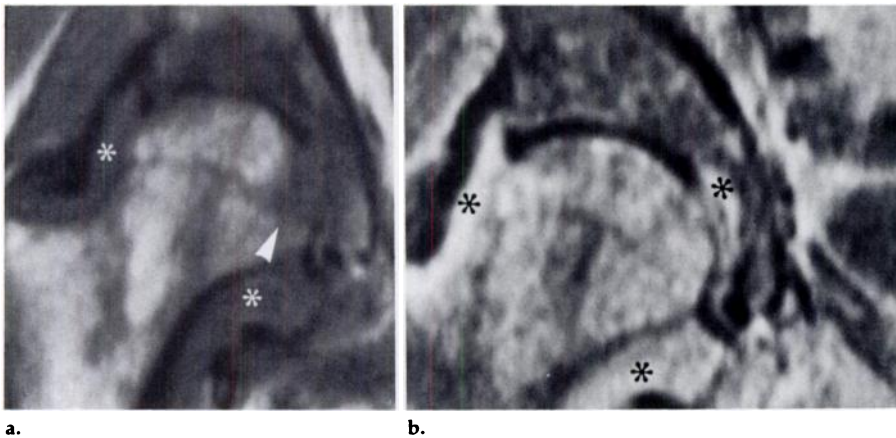

Figure 3. MR images in 45-year-old man with septic hip, confirmed by joint aspiration, and aplastic anemia. (a) Coronal image (SE 499/28) depicts ill-defined intermediate signal intensity present in medial aspect of femoral head (arrowhead) extending below fovea capitis and acetabulum. Distended joint capsule (*) due to exudate manifests intermediate signal intensity. (b) Coronal image (SE 1,999/56) discloses high signal intensity of exudate (*) distending capsule and medial joint space. High signal intensity of medial aspect of femoral head is due to osteomyelitis and corresponds to area shown in a. Signal intensity of acetabulum remains relatively low compared with that of femoral head, suggesting change in marrow consistent with myelofibrosis known to be affecting patient.
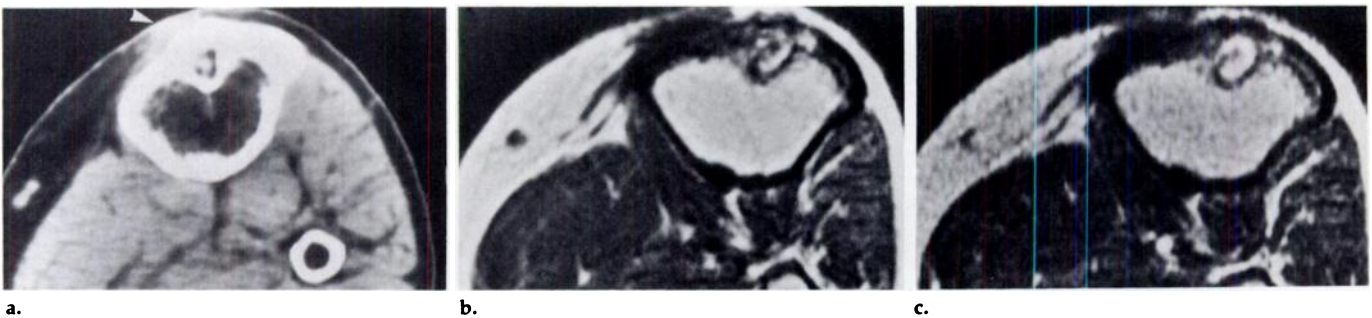
normal signal changes were present in the medullary cavity or soft tissue. However, a severely narrowed first tarsometatarsal joint, as shown on radiographs, appeared on T2-weighted images as a distinct zone of low-intensity signal in comparison with the contralateral normal joint.

Soft-tissue infection (four patients).— The underlying medullary signal appeared normal. The signal intensity of foci of cellulitis in three patients was similar to that of the inflamed soft tissue adjacent to foci of osteomyelitis (low intensity in T1-weighted images and high intensity on T2-weighted images), and the margins of the lesions were similarly ill defined. A soft-tissue abscess was well marginated (Fig. 6).

Old fracture without infection (one patient).—The bone of a healed tibial fracture appeared as a heterogeneous low-to-intermediate intensity signal on T1-weighted images and had slightly increased intensity on T2-weighted images. No focus of high signal intensity was detected. The pin tracks and thickened cortex remained of low signal intensity on both T1- and T2-weighted sequences.

Gaucher disease with medullary infarcts (one patient).—The infarcts were characterized by discrete inhomogeneous rings of low signal intensity surrounding highly intense cores on T1-weighted images. No significant change in signal intensity was seen on T2-weighted images. There was no evidence on MR images of fluid in the knee, and the soft tissue was normal.

DISCUSSION

On the basis of current concepts of the pathophysiology of osteomyelitis (17), the changing pattern of MR signal intensity can be explained as follows: In acute osteomyelitis, because of an increase in intramedullary water caused by edema, exudate, hyperemia, and ischemia, the infected marrow manifests low signal intensity on T1-weight-

Figure 4. Images in a 30-year-old man with chronic osteomyelitis and sequestrum of proximal tibia resulting from infected distal tibial fracture 6 years earlier. (a) CT scan of proximal tibia. Rod track is bounded by sclerotic rim and contains central sequestrum. Irregularly thickened cortex and increased density of pretibial soft tissue (arrowhead) are present. (b) Axial MR image at same level (SE 500/28). Irregular area of abnormally low signal intensity is present in tibia and pretibial soft tissue. (c) On axial MR image (SE 1,500/56) bright, high-intensity abscess with central dark sequestrum and outer dark rim of sclerotic bone. Soft-tissue signal remains unchanged, indicating absence of active infection and presence of scar tissue.

a.   b.   c.
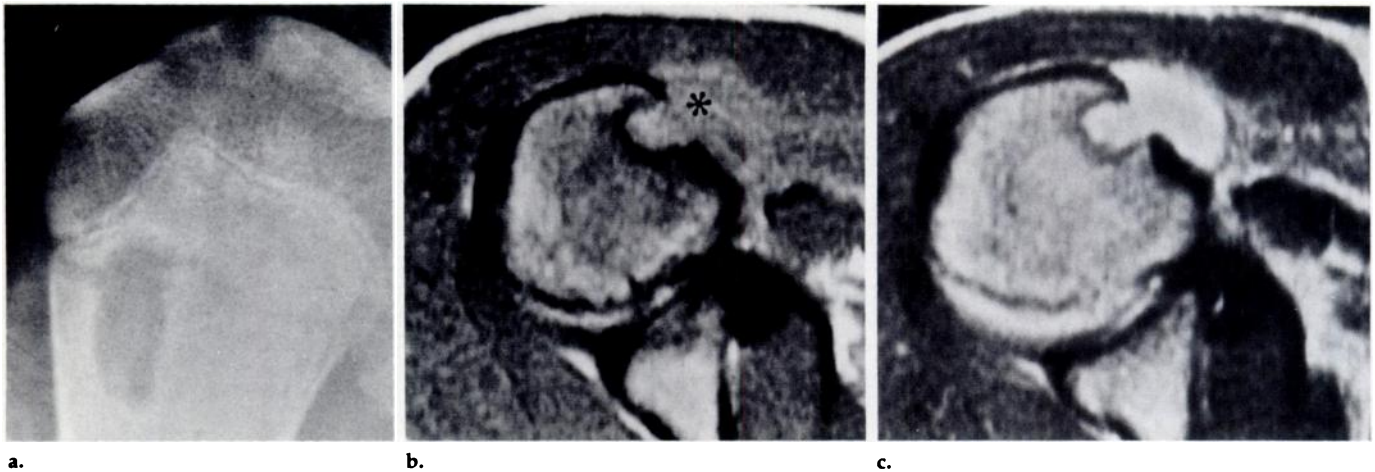
Figure 5. Images in a 15-year-old boy with subacute osteomyelitis and Brodie abscess of humerus. (a) Plain radiograph shows metaphyseal cavity. (b) Axial MR image (SE 500/20), reveals well-defined, relatively high-intensity lesion outlined by low-intensity rim in anterior aspect of humeral neck. Soft tissue (∗) adjacent to bone lesion is ill defined and of abnormally high signal intensity. (c) Axial MR image (SE 1,500/56) reveals very bright signal typical of Brodie abscess with soft-tissue extension.

ed images, becoming high in intensity on T2-weighted images. During this early stage the margins of the lesions are usually ill defined. With further localized bone destruction, the margins tend to become more distinct. The histologic changes of resolved or resolving infections reflect the resolution of both inflammatory exudate and secondary ischemia. Unless there is complete restitution and remodeling of the bone, as may occur in infants and children, healing usually results in fibrosis and irregular overgrowth of bone, resulting in a lower proton density and shorter T2 values. Fracture or surgery, with reactive sclerosing new bone formation and fibrosis within the medullary canal, leads to replacement of the normal marrow in an uneven pattern, appearing on MR images as areas of mixed low, intermediate, and high signal intensities that are relatively constant on T1- and T2-weighted sequences.

Sequestra are isolated fragments of devitalized bone, usually cortical, surrounded by exudate. On MR images, the signal intensity of a sequestrum is similar to that of the bone from which it is derived, that is, low intensity if cortical bone and higher intensity if cancellous bone. If active infection is present in association with chronic osteomyelitis, the exudate tends to manifest low signal intensity on T1-weighted images, may surround a low-intensity or high-intensity sequestrum, and tends to increase in intensity on T2-weighted images.

In subacute osteomyelitis with Brodie abscess, the abscess is often surrounded by a thick, sclerotic rim. The abscess may rarely breach the cortex and extend extraosseously. Associated sequestra are uncommon. In our limited series of cases, the signal intensity

of a Brodie abscess tended to be low to intermediate on T1-weighted images and very high on T2-weighted images. The signal is homogeneous and sharply outlined by a thick, low-intensity rim on both T1- and T2-weighted images.

In septic arthritis, intrarticular effusion (or exudate) and destruction of articular cartilage, with or without subchondral bone involvement, are the major pathologic changes. MR imaging is very sensitive in the depiction of increased joint fluid (16) and medullary bone destruction. Destruction of the articular cartilage results in loss of its normal intermediate-intensity signal. Because the destroyed articular cartilage leaves the joint bounded only by subchondral cortical bone, the joint space appears to be of lower signal intensity and more distinct on T2-weighted images than it does normally. If there is no medullary involvement, the MR imaging pattern is similar to that of any noninfectious inflammatory, traumatic, or degenerative arthritis.

Because the inflammatory soft-tissue changes associated with osteomyelitis have histologic and morphologic features identical to those of the affected bone, their signal intensities are similar. On T1-weighted images, the normally high-intensity signal of subcutaneous fat and intermuscular fatty septa is replaced by the intermediate signal intensity of the inflammatory infiltrate. In the absence of an abscess, the margins of the infiltrate are ill defined. Scarring of the soft tissue after trauma or surgery and healed inflammation appear as areas of low-to-intermediate signal intensity on both T1- and T2-weighted images.

As for the differential diagnosis, malignant bone tumors tend to manifest a well-demarcated, inhomogeneous intraosseous component and, when local-

ly advanced, a well-defined extraosseous soft-tissue component (18, 19). Although the signal intensity of most bone tumors is similar to that of osteomyelitis, the morphologic features observed in our series of osteomyelitis cases differ from those previously described in bone tumors and may prove a useful guide to differential diagnosis.

In this study, MR imaging allowed successful identification of all ten cases of osteomyelitis and four cases of soft-tissue infection without bone involvement. The possibility of active infection in another three patients was excluded with MR imaging, even though one of them had positive findings on a radionuclide bone scan and another had a past history of osteomyelitis.

Although T1-weighted images were very sensitive in depicting pathologic lesions of medullary bone and adipose tissue, they exhibited no pathognomonic changes of active infection. Only when the abnormally low-intensity signal on T1-weighted images changed to a high-intensity signal on T2-weighted images, even brighter than that of normal marrow or fat, was an active infectious process strongly suggested. Therefore, both T1- and T2-weighted sequences are needed to evaluate musculoskeletal infection. One of the advantages of MR imaging is its capability of providing multiplanar images. For imaging the extremities, we found that axial images were capable of demonstrating the most detailed depiction of intra- and extraosseous pathologic conditions, particularly in complicated cases of chronic osteomyelitis and in small, thin bones. Coronal images were best for studying joints. However, to fully appreciate the true extent of disease, images in multiple planes were required.
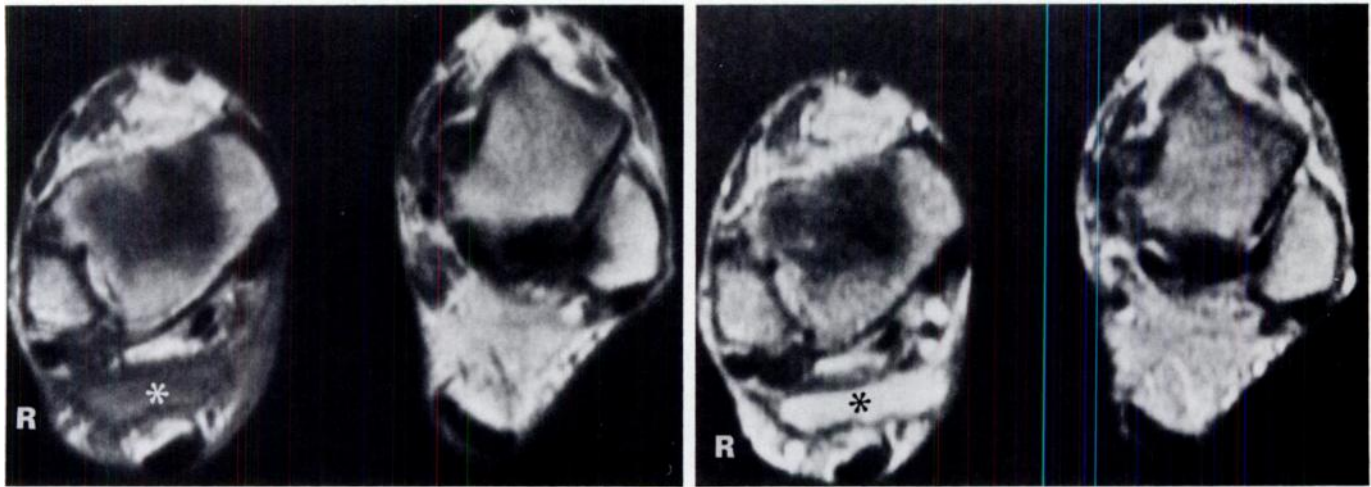
a. **b.**

Figure 6. Axial MR images in a 50-year-old man with soft-tissue abscess of right ankle. **(a)** SE 500/28 image depicts fairly well-defined abscess of intermediate signal intensity (∗) anterior to Achilles tendon. Diffuse areas of intermediate signal intensity are present in adjacent skin (compare with contralateral normal ankle). **(b)** On SE 2,000/84 image soft-tissue abscess (∗) is very bright, well demarcated, and covered by bright edematous subcutaneous fat and skin. Underlying bone is normal.

When compared with the various radionuclide studies, MR imaging has been reported to have equivalent sensitivity for osteomyelitis of the vertebrae or extremities (3, 4, 9, 10, 12). Certain advantages of MR imaging over radionuclide studies include greater accuracy in delineating the extent of disease, more rapid evaluation, and elimination of the need for an intravenous injection or ionizing radiation. In our study, MR imaging was 100% accurate in depicting active osteomyelitis, while Tc-99m bone scans produced three false-positive and one false-negative result, and In-111 leukocyte scans yielded one false-negative result.

CT scans were obtained in both cases of chronic osteomyelitis associated with previous fractures and orthopedic surgery, and in one of the two cases of Brodie abscess. As in several published reports (5–7), CT was able to disclose sequestra and sinus tracts. However, the results of CT in our two cases of chronic osteomyelitis were equivocal for active infection. Indeed, we found MR imaging to be superior to CT in these cases because it was able to disclose not only sequestra and sinus tracts but also sites of active infection in bone and soft tissue. It has been reported that MR imaging is more sensitive than CT in the detection of infected metal implants (4). However, the greater spatial resolution currently featured by CT continues to make it invaluable for the depiction of small sequestra, foreign bodies, and subtle foci of gas.

To summarize, we found that MR imaging had high sensitivity and specificity in the detection of active infection

in bone, even in cases of chronic osteomyelitis with or without previous surgery or fracture. Because it is capable of providing detailed anatomic information regarding the extent of pathologic change, MR imaging may be the most accurate imaging modality in differentiating osteomyelitis from septic arthritis or soft-tissue infection. It would seem ideal for guiding biopsy and surgery. Two limitations of our study are that surgical confirmation was obtained in only 12 of the 17 cases, and that the MR pulse sequence protocols were inconsistent. Future, more standardized studies on a larger scale with more advanced technology should serve to confirm the usefulness of MR imaging in the evaluation of musculoskeletal infections. ■

References

1. Lewin JS, Rosenfield NS, Hoffer PB, Downing D. Acute osteomyelitis in children: combined Tc-99m and Ga-67 imaging. Radiology 1986; 158:795–804.
2. Tumeh SS, Aliabadi PA, Weissman BN, McNeil BJ. Chronic osteomyelitis: bone and gallium scan patterns associated with active disease. Radiology 1986; 158:685–688.
3. Modic MT, Pflanze W, Feiglin DHI, Belhobek G. Magnetic resonance imaging of musculoskeletal infections. Radiol Clin North Am 1986; 24:247–258.
4. Berquist TH, Brown ML, Fitzgerald RH, May GR. Magnetic resonance imaging: application in musculoskeletal infection. Magn Reson Imaging 1985; 3:219–230.
5. Azouz EM. Computed tomography in bone and joint infections. J Can Assoc Radiol 1981; 32:102–106.
6. Wing VW, Jeffrey RB, Federle MP, Helms CA, Trafton P. Chronic osteomyelitis examined by CT. Radiology 1985; 154:171–174.
7. Ram PC, Martinez S, Korobkin M, Breiman RS, Gallis HR, Harrelson JM. CT detection of intraosseous gas: a new sign of osteomyelitis. AJR 1981; 137:721–723.
8. Reis ND, Lanir A, Benmair J, Hadar H. Magnetic resonance imaging in orthopaedic surgery. J Bone Joint Surg [Br] 1985; 67:659–664.
9. Atlan H, Sigal R, Hadar H, et al. Nuclear magnetic resonance proton imaging of bone pathology. J Nucl Med 1986; 27:207–215.
10. Barry D, Scoles PV, Nelson AD. Osteomyelitis in children: detection by magnetic resonance. Radiology 1984; 150:57–60.
11. Modic MT, Pavlicek WP, Weinstein MA, et al. Magnetic resonance imaging of intervertebral disk disease. Radiology 1984; 152:103–111.
12. Modic MT, Feiglin DH, Piraino DW, et al. Vertebral osteomyelitis: assessment using MR. Radiology 1985; 157:157–166.
13. Smith FW, Runge V, Permezel M, Smith CC. Nuclear magnetic resonance (NMR) imaging in the diagnosis of spinal osteomyelitis. Magn Reson Imaging 1984; 2:53–56.
14. de Roos A, van Persijn van Meerten EL, Bloem JL, Bluemm RG. MRI of tuberculous spondylitis. AJR 1986; 147:79–82.
15. Paushter DM, Modic MT, Masaryk TJ. Magnetic resonance imaging of the spine: applications and limitations. Radiol Clin North Am 1985; 23:551–562.
16. Beltran J, Noto AM, Herman LJ, Mosure JC, Burk JM. Christoforidis AJ. Joint effusions: MR imaging. Radiology 1986; 158:133–137.
17. Bonakdar-pour A, Gaines VD. The radiology of osteomyelitis. Orthop Clin North Am 1983; 14:21–37.
18. Zimmer WD, Berquist TH, McLeod RA, et al. Bone tumors: magnetic resonance imaging versus computed tomography. Radiology 1985; 155:709–718.
19. Vanel D, Di Paola R, Contesso G. Magnetic resonance imaging in musculoskeletal primary malignant tumors. In: Magnetic resonance annual. New York: Raven, 1987; 237–261.